Materials and Design 52 (2013) 452–458

Contents lists available at SciVerse ScienceDirect

Materials and Design

journal homepage: www.elsevier.com/locate/matdes

Short Communication

Influence of overlapping tracks on microstructure evolution and corrosion behavior in laser-melt magnesium alloy

Y.C. Guan [a,b,*], W. Zhou [a,b], Z.L. Li [b], H.Y. Zheng [b]

[a] Nanyang Technological University, 50 Nanyang Avenue, Singapore 639798, Singapore
[b] Singapore Institute of Manufacturing Technology, 71 Nanyang Drive, Singapore 638075, Singapore

ARTICLE INFO

Article history:
Received 28 March 2013
Accepted 24 May 2013
Available online 4 June 2013

ABSTRACT

Overlapping of laser beam tracks has significant influence on surface quality of laser-treated materials. This paper examines how overlapping tracks affect heat flow, solidification microstructure and electrochemical behavior of laser-melt magnesium alloy. Microstructure evolution of laser-melt surface with different overlapping rates at optimized scanning speed is investigated. Results show that solidification microstructure changes from cellular grains to cellular–dendritic and equiaxed dendritic in the overlapped area when overlapping rate increases. Numerical model suggests that Marangoni convection plays a predominate role in determining the solidification microstructure, and it increases significantly with the overlapping rate. The effect of microstructure in-homogeneities caused by overlapping on electrochemical behavior has also been analyzed.

1. Introduction

Laser processing has recently generated intense research activities on improving surface properties of materials. Previous researchers have found that surface performance of metallic alloys, such as wear and corrosion resistance, is enhanced remarkably due to refined microstructure and enriched alloying elements following rapid solidification associated with the laser processing [1–9]. Mazumder and his co-workers [4,5] have investigated effect of laser-cladding technique upon the microstructure and the corrosion resistance of treated materials, and found that corrosion properties of the laser claddings has been improved significantly compared with that of commercially used materials. Gray and Luan [6] have reviewed various techniques for protective coatings on magnesium alloys due to poor surface properties, and suggested laser processing is a very promising method for Mg alloys to extend their industrial applications. Audebert et al. [7] have examined the ability of production of glassy metallic layers on Zr- and Mg-based alloys by laser surface treatment. Man et al. [8] have suggested that laser modification technique employed in their study is capable of enhancing the feasibility and biocompatibility of NiTi samples used as orthopedic implants mainly due to improved wear resistance. Most recently, Sun et al. [9] have studied laser surface alloying to form wear resistant layers on steel rolls with powders, and concluded that the improvement in wear resistance is attributed to combined results of grain refining and solution strengthening effect.

In order to apply laser techniques for large surface components in real engineering applications, overlapping adjacent traces as a result of multiple passes using scanning laser beam is usually necessary for production of area coverage. It has long been realized that laser beam overlapping may play a significant role in influencing the final surface properties of laser-treated materials [1–3]. Lewis and Schlienger [10] have considered that overlapping plays an important role in determining quality control during laser assisted direct metal deposition. Particularly, overlapping is important in determining corrosion resistance due to microstructure in-homogeneities in the molten pool [11–16]. Liu et al. [11] have demonstrated that overlapping results in microstructural non-uniformity within re-heated and re-melted area, which leads to preferred sites for corrosion development. Reitz and Rawers [12] have observed that accelerated corrosion occurs near laser beam overlap region, and iron element segregated near periphery of each molten pool is responsible for accelerated corrosion in zirconium alloys. Virtanen et al. [13] have showed that pits are initiated along the overlapped area of laser traces after surface melting of Al–7Si and Al–12Si cast alloys. Conde et al. [14] have reported that corrosion resistance of laser-melt steels depends critically on laser processing parameters, and care must be taken in the choice of parameters that leads to optimal properties in each material. In our previous work, coarse structure of laser-melt AZ91D Mg alloy is investigated in the overlapped area caused by scanning speed, and it provides preferential site for pitting corrosion in simulated body fluid [15,16].

---

[*] Corresponding author at: Singapore Institute of Manufacturing Technology, 71 Nanyang Drive, Singapore 638075, Singapore. Tel.: +65 6793 8386; fax: +65 6791 6377.

E-mail address: guan0013@e.ntu.edu.sg (Y.C. Guan).

0261-3069/$ - see front matter © 2013 Elsevier Ltd. All rights reserved.
http://dx.doi.org/10.1016/j.matdes.2013.05.075

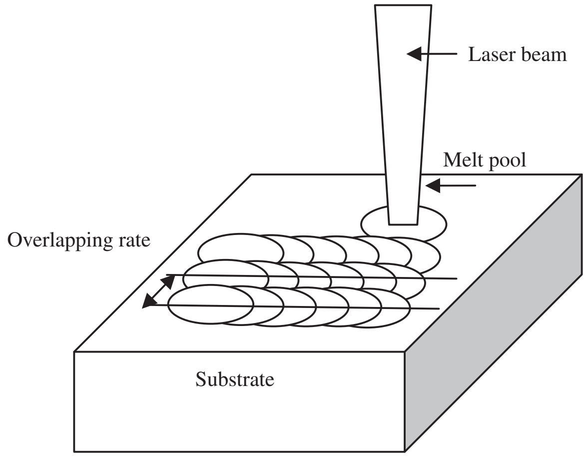

Fig. 1. Schematic diagram of laser surface melting process.

However, as of now, there has been no concentrated effort to study the effect of laser beam overlapping on kinetics of solidification microstructure evolution in the molten pool. The objective of this research is to study how overlapping tracks affect heat transfer and liquid flow, microstructure evolution as well as electrochemical behavior of laser melting AZ91D Mg alloy at optimized scanning speed. The heat transport mechanism in the molten pool was analyzed from a well-tested numerical heat transfer and fluid flow model by DebRoy and Yang [17–19].

2. Materials and methods

The material studied was an as-cast AZ91D Mg alloy with the following chemical composition (wt%): Al 8.97, Zn 0.78, Mn 0.31, Si 0.023, Cu 0.002, Ni 0.0005 and Mg balance. The specimens of 20 mm by 30 mm by 3 mm were extracted from the ingot, ground with progressively finer SiC paper (180, 400, 800, 1200, 2400 and 4000 grit), cleaned with alcohol, and then irradiated with Lumonics JK702 Nd:YAG laser system (with wavelength of 1064 nm) under high purity Ar gas protection. The fixed laser parameters were power density 3.82×10^4 W/cm^2, scanning speed 10 mm/s, frequency 100 Hz, and pulse duration 1 ms. Overlapping rate was varied from 25% to 90% during laser processing, as shown in Fig. 1. Four specimens marked as E, F, G and H were chosen in this paper, as the overlapping rates were 25%, 50%, 75% and 90%, respectively. The laser was operated in a near TEM$_{00}$ mode and the beam was defocused to 1 mm in diameter (the distance between two subsequent tracks was around 500 μm).

Microstructural features of the specimens were studied using a Zesis optical microscope, a JEOL 5600 LV SEM equipped with an energy-dispersive X-ray spectrometer (EDS), and JEOL 2010 TEM. The EDS measurements provided information on the chemical composition. The electrochemical behavior of as-received and laser-irradiated AZ91D specimens was studied using a potentiostat/galvanostat corrosion measurement system (EG&G model 263A) following procedures of ASTM: G59-97(2009) for Conducting Potentiodynamic Polarization Resistance Measurements [15]. The specimens were immersed in the 150 ml of 3.5% NaCl solution with a pH of 7.25. The exposed area was about 1 cm^2, and a polarization scan was carried out at a rate of 0.8 mV s^{-1}.

3. Results

Figs. 2 and 3 indicate top view of microstructure evolution at AZ91D Mg alloy surface before and after laser melting by SEM and TEM, respectively. As shown in Fig. 2a, microstructure of as-received AZ91D Mg alloy contained bulk and lamellar β-Mg$_{17}$Al$_{12}$ phase distributed non-homogeneously in a matrix of α-Mg grains. After laser surface melting, solidification microstructure consisted of typical cellular/dendrite structure was observed in the molten pool, which was derived from refined α-Mg and β-Mg$_{17}$Al$_{12}$ phases according to previous study [15,16]. Coarse structure was formed in the overlapped area along laser tracks, and the amount and size of such structure increased significantly with the laser overlapping rates, as shown in Fig. 2b–e. These coarse structures were further investigated in Fig. 2 shown as the high magnification images. At low overlapping rate, fine cellular structure with size of 2–3 μm were observed in the overlapped area, and small solidification cracks were also found in the microstructure, as shown in Fig. 2b. When the overlapping rate increased from 25% to 75%, cellular structure to dendrite structure transition took place near solidification front at the periphery of each molten pool, and more dendrite was found in the overlapped area, as shown in Fig. 2c and d. At high overlap rate as 90%, coarse equiaxed dendrite structure was formed, as shown in Fig. 2e.

Quantitative analyses of chemical compositions based on EDS measurement found that with the increasing overlapping rates, average Al concentration in the overlapped area increased from 11.5 wt% to 16.7 wt%, whereas average Mg concentration decreased from 87.1 wt% to 82.2 wt% simultaneously. The reason for the chemical compositions change was due to enhanced selective vaporization of alloying elements with the increasing overlapping rates during laser processing [3,15,16].

Fig. 3a reveals thin plate shape of β-Mg$_{17}$Al$_{12}$ phase in the as-received surface. After laser melting, morphology of β-Mg$_{17}$Al$_{12}$ phase changed significantly to cellular/dendrite structure as well as nano-sized particles, as shown in Fig. 3b–d. The evolution of these structures was in agreement of SEM observations. It should be noted that nano-sized particles were identified as β-Mg$_{17}$Al$_{12}$ precipitates according to further investigation of orientation relationship between the particles and α-Mg matrix. With the overlapping rate increases, a driving force tends to make dispersions of small crystals coarsening as a result of "quench–hold–quench" process [1,16]. Correspondingly, tiny precipitates shrink and eventually vanish together, while large precipitates grow at their expense by solid-state diffusion during coarsening, leading to cluster-shaped particles in the microstructure. On the other hand, at 90% overlapping rate, strong selective vaporization of Mg and Al elements occurs due to accumulated high laser energy, resulting in Al enriched significantly in the laser-melt layer. The high density of enlarged and gathered particles as well as increased Al concentration would increase the volume fraction of brittle β-Mg$_{17}$Al$_{12}$ phase, the melt layer also becomes increasingly brittle [20]. Therefore, TEM result of specimen with 90% overlapping rate is missing because it was too brittle to break into pieces during sample preparation process.

Cross-section views of molten pool in the laser-melt specimens were investigated in Figs. 4 and 5. With the increasing overlapping rates, bottom morphology of the molten pool became flat, but melt depth kept as nearly 150 μm for all molten pools. Small solidification cracks were also found at low overlapping rate in the molten pool, as shown in Fig. 4a. Further investigation was observed using SEM. At low overlapping rate, fine cellular structure was found in the end of previous laser trace, and needle-shape dendrite structure was formed along the laser trace, as shown in Fig. 5a and b. Fig. 5a and b also show that few cellular/dendrite structures were found in the non-overlapped area of the molten pool. When overlapping rate was increased, coarse equiaxed dendritic structures replaced fine cellular and cellular–dendrite structure in the overlapped area, and the solidification microstructure in the molten pool became much more homogenous, as shown in Fig. 5c and d.

Polarization study of as-received material and laser-melt surfaces with different overlapping rates was further analyzed in